Landes Bioscience www.landesbioscience.com

Supplemental Material to:

Michelle Cicchini, Rumela Chakrabarti, Sameera Kongara, Sandy Price, Ritu Nahar, Fred Lozy, Hua Zhong, Alexei Vazquez, Yibin Kang, and Vassiliki Karantza

Autophagy regulator BECN1 suppresses mammary tumorigenesis driven by WNT1 activation and following parity

Autophagy 2014; 10(11)
http://dx.doi.org/10.4161/auto.34398

www.landesbioscience.com/journals/autophagy/article/34398

Cicchini_Suppl Fig1

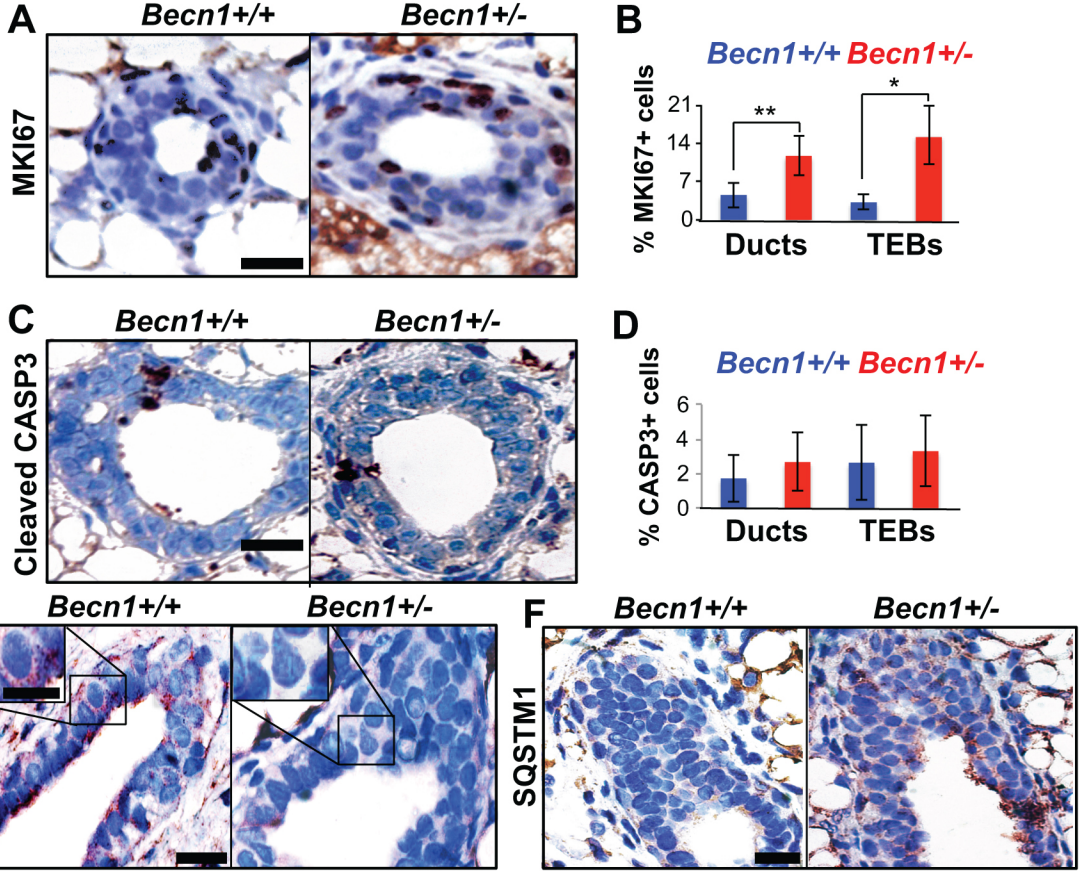

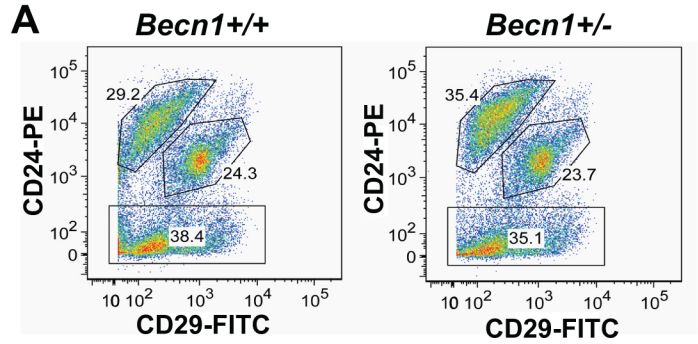
A
Becn1+/+
Becn1+/-
CD24-PE
CD29-FITC
29.2
24.3
38.4
35.4
23.7
35.1

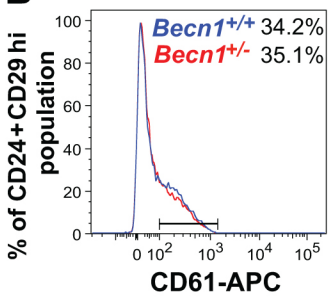
B
Becn1+/+ 34.2%
Becn1+/- 35.1%
% of CD24+CD29 hi population
CD61-APC

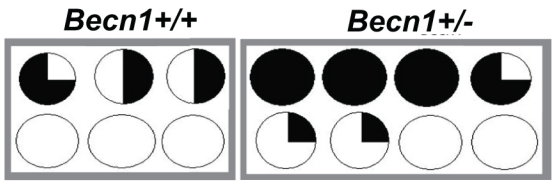
C
Becn1+/+
Becn1+/-

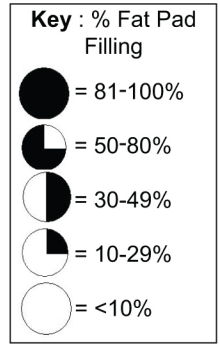
Key : % Fat Pad Filling
= 81-100%
= 50-80%
= 30-49%
= 10-29%
= <10%

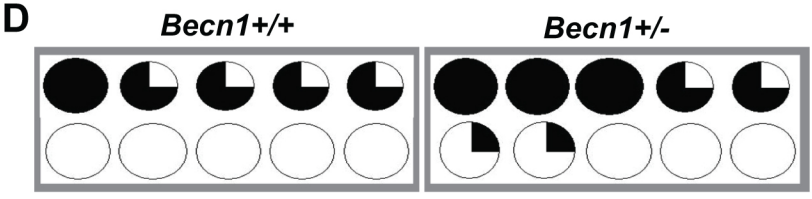
D
Becn1+/+
Becn1+/-

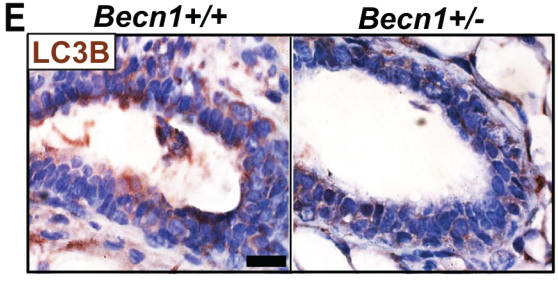
E
Becn1+/+
Becn1+/-
LC3B

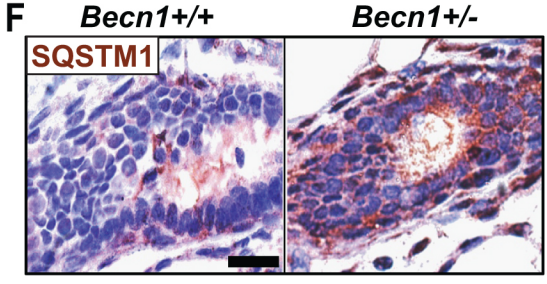
F
Becn1+/+
Becn1+/-
SQSTM1

Cicchini_Suppl Fig 3

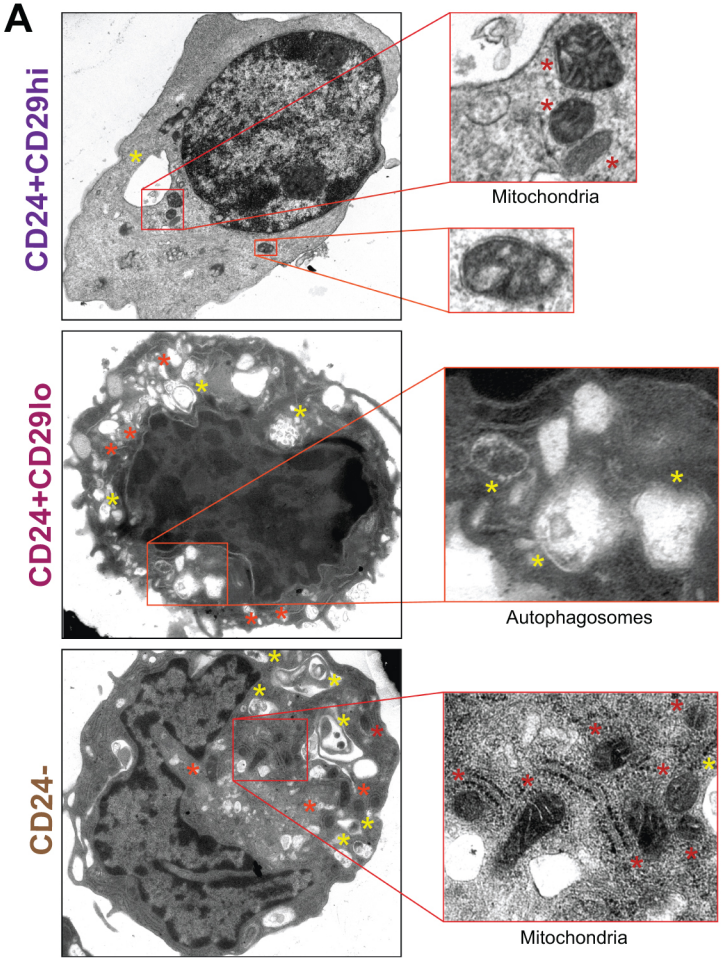

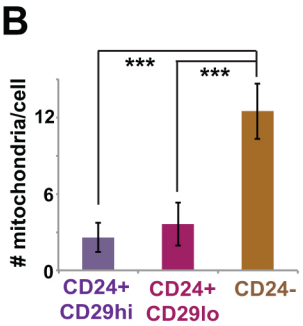

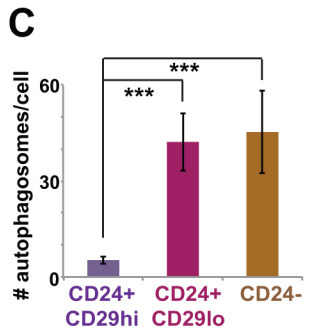

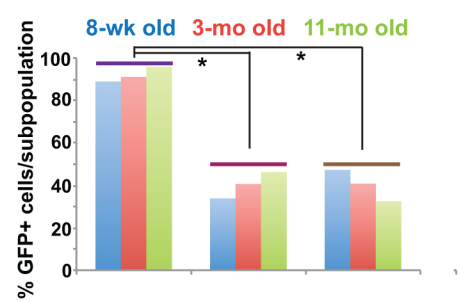

Cicchini_Suppl Fig 4

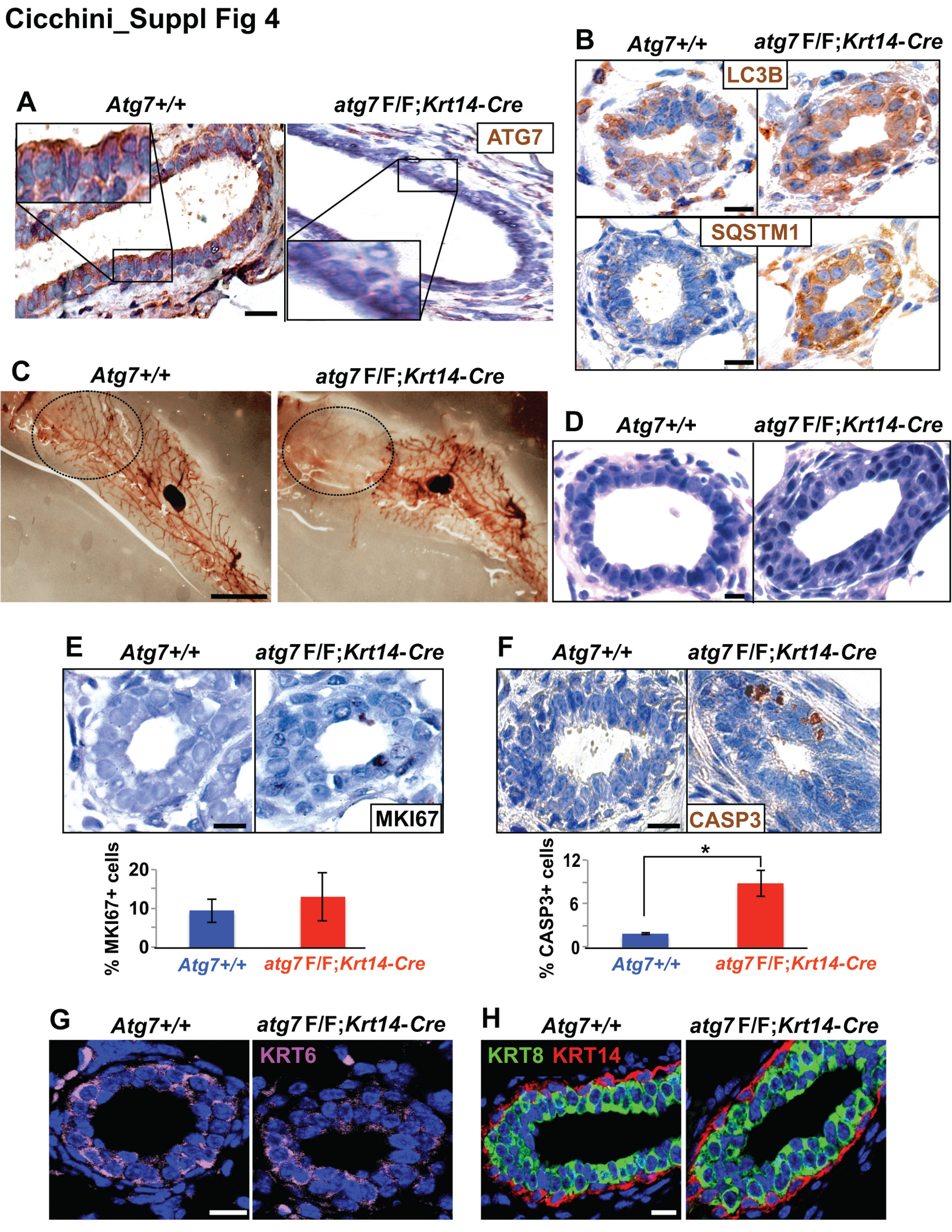

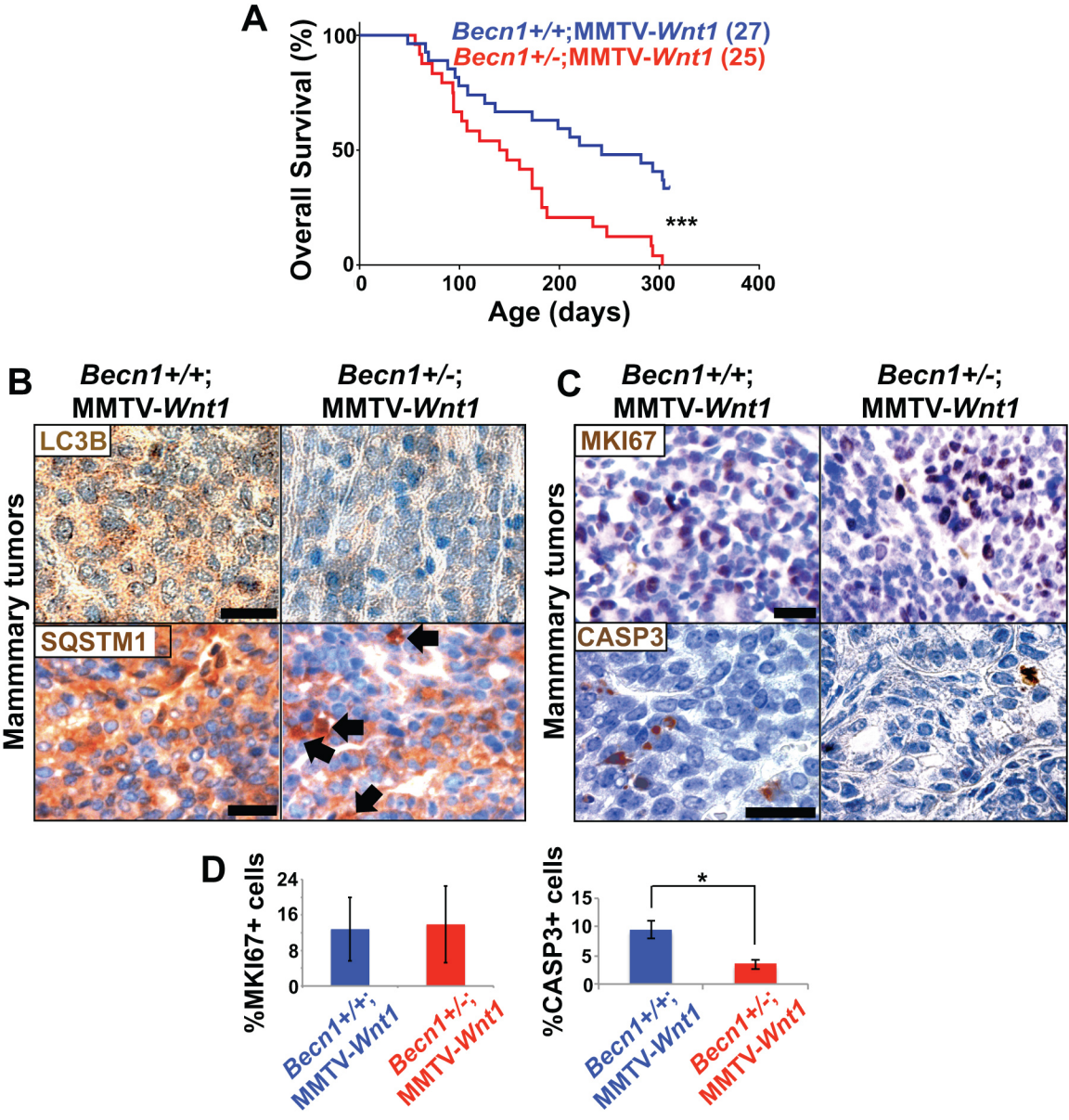
A
Becn1+/+;MMTV-Wnt1 (27)
Becn1+/-;MMTV-Wnt1 (25)
Overall Survival (%)
100
50
0
***
0
100
200
300
400
Age (days)
B
Becn1+/+; MMTV-Wnt1
Becn1+/-; MMTV-Wnt1
Mammmary tumors
LC3B
SQSTM1
C
Becn1+/+; MMTV-Wnt1
Becn1+/-; MMTV-Wnt1
Mammmary tumors
MKI67
CASP3
D
%MKI67+ cells
24
16
8
0
Becn1+/+; MMTV-Wnt1
Becn1+/-; MMTV-Wnt1
%CASP3+ cells
15
10
5
0
*
Becn1+/+; MMTV-Wnt1
Becn1+/-; MMTV-Wnt1

Cicchini_Supp Figure 6

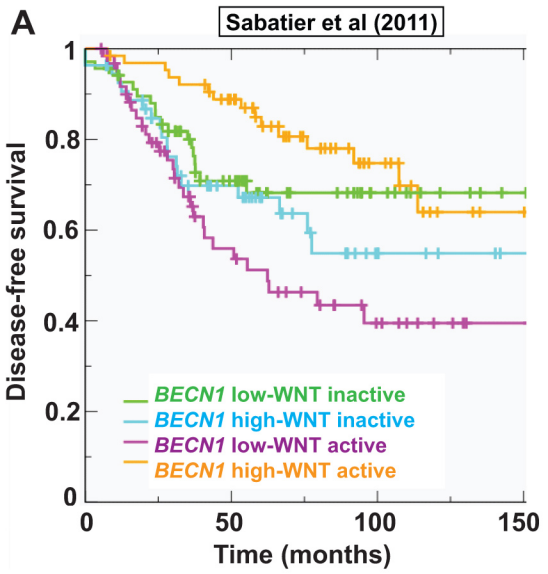

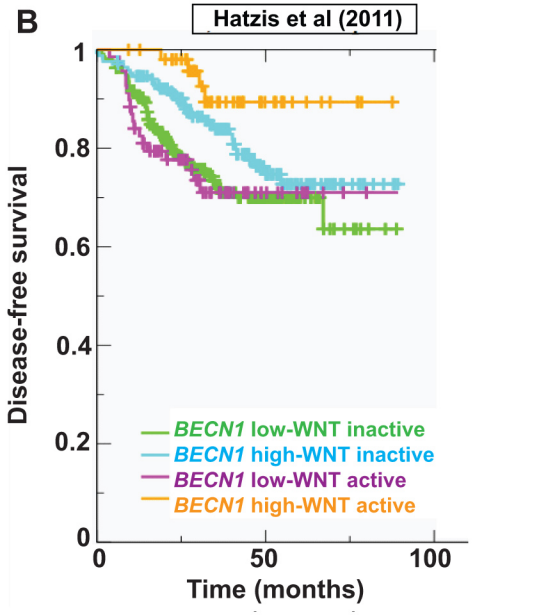

Figure S1. MGs of *Becn1*$^{+/-}$ mice display increased proliferation and defective autophagy status. (**A, C, E and F**) Immunohistochemical analysis of MGs from cohoused *Becn1*$^{+/+}$ (left) and *Becn1*$^{+/-}$ (right) 5-wk old littermates. (**A**) Representative images and (**B**) quantification of MKI67^{+} cells in mammary ducts (left) and TEBs (right) shown as means ± SDs (n=3 mammary gland specimens per genotype). (**C**) Representative images and (**D**) quantification of cleaved CASP3 in each sample in TEBs and ducts shown as means ± SDs (n=3 mammary gland specimens per genotype). (**E**) Representative image of LC3B staining confirms decreased LC3B puncta in MGs from *Becn1*$^{+/-}$ mice. (**F**) Representative image of SQSTM1 staining confirms accumulation of SQSTM1 in MGs from *Becn1*$^{+/-}$ mice. **P* <0.05 and ***P* <0.01 by a two-tailed Student t test. Scale bar = 30 μm for (**A,C,E,F**).

Figure S2. Outgrowths from CD24^{+}CD29^{hi} *Becn1*$^{+/-}$ MEC transplantation exhibit increased MaSC activity and retain defective autophagy status. (**A and B**) MEC sorting experiments were performed 5 independent times. (**A**) FACS was performed on freshly isolated MECs stained with PI, LIN (CD31, CD45, and LY76), CD24, and CD29. Images are representative of *Becn1*$^{+/+}$ (left) and *Becn1*$^{+/-}$ (right) MEC distribution with gating for PI^{-}LIN^{-} cells and based on CD24 and CD29 expression. No significant differences were seen in relative MEC subpopulations. (**B**) A representative histogram shows similar numbers of CD61^{+} cells between *Becn1*$^{+/+}$ and *Becn1*$^{+/-}$ CD24^{+}CD29^{hi} MEC populations. (**C and D**) Circles represent fat pads and the black color represents the percentage of the

mammary fat pad that is filled in. (**C**) Increased repopulation frequency and mammary fat pad filling are seen following transplantation of 500 $CD24^{+}CD29^{hi}$ MECs isolated from 8 wk old *Becn1*$^{+/-}$ mice, contralateral $CD24^{+}CD29^{hi}$ *Becn1*$^{+/+}$ and *Becn1*$^{+/-}$ MEC transplantations were performed. (**D**) Increased repopulation frequency and mammary fat pad filling are seen following transplantation of 500 $CD24^{+}CD29^{hi}$ MECs isolated from 9.5-wk old *Becn1*$^{+/-}$ mice, contralateral $CD24^{+}CD29^{hi}$ *Becn1*$^{+/+}$ and *Becn1*$^{+/-}$ MEC transplantations were performed. (**E**) Representative image of LC3B staining in samples confirms decreased LC3B puncta in outgrowths from $CD24^{+}CD29^{hi}$ *Becn1*$^{+/-}$ MEC transplantation. (**F**) Representative image of SQSTM1 staining confirms accumulation of SQSTM1 in outgrowths from $CD24^{+}CD29^{hi}$ *Becn1*$^{+/-}$ MEC transplantation. Scale bar= 30 μm for (**E,F**).

Figure S3. FACS for CD24 and CD29 expression defines MEC populations with different autophagy levels. $PI^{-}LIN^{-}$ MECs were isolated by FACS based on CD24 and CD29 expression, and examined by EM. ^ and * denote mitochondria and autophagosomes, respectively.

Figure S4. *Krt14*-driven conditional biallelic *Atg7* deletion confers autophagy deficiency in the mammary gland. (**A to H**) Evaluation of MGs from *Atg7*$^{+/+}$ (left) and *atg7*$^{F/F}$;*Krt14-Cre* (right) mice. (**A**) Representative images of ATG7 staining confirms *Atg7* deletion in MGs from *atg7*$^{F/F}$;*Krt14-Cre* mice. (**B**) Representative images of SQSTM1 (top) and LC3B (bottom) staining. (**C**) Representative MG

whole mounts (WM) from 6.5-wk old mice reveal decreased mammary fat pad filling in MGs from *atg7*$^{F/F}$;*Krt14-Cre* mice. (**D**) Representative images of hematoxylin and eosin (H&E) staining reveal similar ductal organization in MGs from *atg7*$^{F/F}$;*Krt14-Cre* and *Atg7*$^{+/+}$ mice. (**E**) Representative images and quantification of MKI67 staining. (**F**) Representative images and quantification of cleaved CASP3 staining. Representative images of (**G**) KRT6 (purple), and (**H**) KRT8 (green) and KRT14 (red) staining. Scale bar = 20 μm for (**A,B,D to H**) and 5 mm for (**C**).

Figure S5. Mammary tumors arising in *Becn1*$^{+/-}$;MMTV-*Wnt1* mice exhibit autophagy-deficient status and decreased apoptosis. (**A**) Kaplan-Meier curves for overall survival in *Becn1*$^{+/+}$;MMTV-*Wnt1* (n=27) and *Becn1*$^{+/-}$;MMTV-*Wnt1* (n=25) mice demonstrates decreased overall survival in *Becn1*$^{+/-}$;MMTV-*Wnt1* mice. (**B and C**) Analysis of mammary tumors arising in *Becn1*$^{+/+}$;MMTV-*Wnt1* (left) and *Becn1*$^{+/-}$;MMTV-*Wnt1* (right) mice. (**B**) Representative image of LC3B staining (top) and SQSTM1 aggregates annotated with arrow (bottom) in tumors from *Becn1*$^{+/-}$;MMTV-*Wnt1* mice. (**C**) Representative image from MKI67 staining (top) and cleaved CASP3 staining (bottom). (**D**) Quantification of MKI67^{+} cells (left) and cleaved CASP3^{+} cells (right) determine proliferation and apoptosis rates, respectively, in tumors. Results are presented as means ± SDs (n=3 mammary tumors per genotype) *P < 0.05 determined by a two-tailed Student t test. Scale bar= 40 μm for (**B,C**).

Figure S6. Kaplan-Meier curves for breast tumors stratified for *BECN1* expression and WNT pathway activation. (**A**) Disease-free survival for patients with breast cancers annotated in the Sabatier cohort. (**B**) Disease-free survival for patients with ERBB2-negative breast cancers annotated in the Hatzis cohort.